

Measurement of electromagnetic tracking error in a navigated breast surgery setup

Vinyas Harish¹, Aidan Baksh¹, Tamas Ungi^{1,2}, Andras Lasso¹, Zachary Baum¹, Gabrielle Gauvin², Jay Engel², John Rudan^{1,2}, Gabor Fichtinger^{1,2}

¹Laboratory for Percutaneous Surgery, Queen's University, Kingston, ON, Canada

²Department of Surgery, Queen's University, Kingston, ON, Canada

ABSTRACT

PURPOSE: The measurement of tracking error is crucial to ensure the safety and feasibility of electromagnetically tracked, image-guided procedures. Measurement should occur in a clinical environment because electromagnetic field distortion depends on positioning relative to the field generator and metal objects. However, we could not find an accessible and open-source system for calibration, error measurement, and visualization. We developed such a system and tested it in a navigated breast surgery setup.

METHODS: A pointer tool was designed for concurrent electromagnetic and optical tracking. Software modules were developed for automatic calibration of the measurement system, real-time error visualization, and analysis. The system was taken to an operating room to test for field distortion in a navigated breast surgery setup. Positional and rotational electromagnetic tracking errors were then calculated using optical tracking as a ground truth.

RESULTS: Our system is quick to set up and can be rapidly deployed. The process from calibration to visualization also only takes a few minutes. Field distortion was measured in the presence of various surgical equipment. Positional and rotational error in a clean field was approximately 0.90 mm and 0.31°. The presence of a surgical table, an electrosurgical cautery, and anesthesia machine increased the error by up to a few tenths of a millimeter and tenth of a degree.

CONCLUSION: In a navigated breast surgery setup, measurement and visualization of tracking error defines a safe working area in the presence of surgical equipment. Our system is available as an extension for the open-source 3D Slicer platform.

KEYWORDS: Quality Assurance System, Electromagnetic Tracking Error, Image-Guided Intervention, Image-Guided Therapy, Visualization, 3D Slicer, SlicerIGT, PLUS Toolkit

1. PURPOSE

Electromagnetic tracking is used in many navigated medical interventions because miniature sensors may be tracked inside the patient without requiring a line of sight. However, electromagnetic tracking becomes inaccurate when the electromagnetic field generated for tracking is distorted by metal objects or other magnetic fields in the workspace. Therefore, the quality of electromagnetic tracking needs to be verified whenever it is used in a new environment.

Various methods have already been developed to monitor electromagnetic tracking error. The methods described by Krücker *et al.* and Feuerstein *et al.* utilize proprietary software. Thus their methods are not easily available for research use or modification^{1,2}. Other methods such as the one described by Lugez *et al.* involve sizeable phantom objects in the surgeon's workspace³. Tracked tools are placed in various well defined slots of the phantoms, and the tracked positions are compared to the known positions. However, phantoms prevent realistic motion of surgical instruments that would represent real procedures and are not sufficiently generic for use in multiple types of procedures. Thus, results obtained using phantoms may be limited. A system is still needed that can measure tracking error during normal tool motions in a complex surgical workflow. Such a system could produce more reliable measurements of tracking error before a navigation system is used in patients.



Figure 1. Highly accurate tracking is crucial when segmenting the tumor in Ungi *et al.*'s lumpectomy workflow (left). Once the tumor is segmented, surgeons are able to view a 3D model of the tumor and operate using a tracked electrosurgical cautery (right).

We have chosen a recently developed surgical navigation system using electromagnetic tracking⁴ as a test subject for our developed quality assurance tool in this study. The LumpNav system is used in breast-conserving surgery, also called lumpectomy. As long as the cancer is staged early, survival rates of lumpectomy are equivalent to mastectomy⁵. Challenges arise during lumpectomy procedures, as most breast cancer tissue types are neither visible, nor palpable for the surgeon. After the surgery, histological analysis is done to determine if cancer-positive margins exist. It is imperative to reduce the likelihood of positive margins since they are associated with two to three times the risk of cancer recurrence⁶. In order to reduce the occurrence of positive margins to 12.5%, Ungi *et al.* generated 3D navigation views to aid surgeons during the excision process⁴. The LumpNav system builds upon the current clinical standard of using a localization wire. The needle used to deploy a hooked wire into the tumor is also electromagnetically tracked, and thus allows for the tracking of the tumor. Once the tumor position is known, electromagnetically tracked ultrasound is used to delineate the margins of the tumor (Figure 1). These margins are then used to generate a 3D model of the tumor that is tracked in real-time, relative to the needle's coordinate system. Concurrent tracking of the cautery guides the surgeon during the excision. Accurate tracking is imperative during the contouring process since the LumpNav system provides audiovisual cues to surgeons to avoid breaching the model generated from the contours (Figure 1). Margins that are too large result in excess tissue being excised, negatively impacting cosmetic appeal post-surgery. Therefore, due to the reliance of the LumpNav system on accurate tracking, it is necessary to assess and visualize the potential tracking error caused by metals and electronic instruments in the workspace before this system is used in a new environment.

2. METHODS

We previously proposed a system for dual-modality tracking for the evaluation of electromagnetic field distortion during crucial moments in a surgical workflow⁷. Our previous system was complicated to use, limited to measuring positional errors, and used manually fabricated hardware components. The implementation is completely open-source, all hardware and software components are freely available and readily usable with a number of different tracking systems.

2.1 Hardware design

In our new system, special hardware tools were designed using the SolidWorks software (2015 SP03, Dassault Systèmes, Vélizy, France) and were 3D printed (Figures 2, 3). A pointer was designed to combine optical markers compatible with the Polaris optical tracker (Northern Digital Inc., ON, Canada) and the 3D Guidance trakSTAR system's (Northern Digital Inc., ON, Canada) electromagnetic sensor. The pointer is modular and has replaceable parts in case of damage (Figure 4) or to accommodate different trackers. It integrates clip-in slots for sensors that are compatible for different systems such as Northern Digital's and Claron's (Toronto, ON, Canada) optical and electromagnetic trackers. An optically tracked reference with a mount that fits on the electromagnetic field generator was also printed under the same design guidelines. The editable design files for both tools are available online, released under a permissive license that allows free usage and modification by users without restrictions (www.plustoolkit.org). The two tracking devices were connected to a laptop running the PlusServer application of the PLUS software toolkit⁸. PlusServer relayed the tracking data to the 3D Slicer (www.slicer.org) application through the OpenIGTLLink communication protocol⁹. Since PLUS supports a wide range of tracking devices, this system can be configured to work with other devices without programming knowledge. An optical tracker, in this case the Northern Digital Inc. Polaris, and dual-modality pointer are brought in the workspace for electromagnetic tracking error measurement.

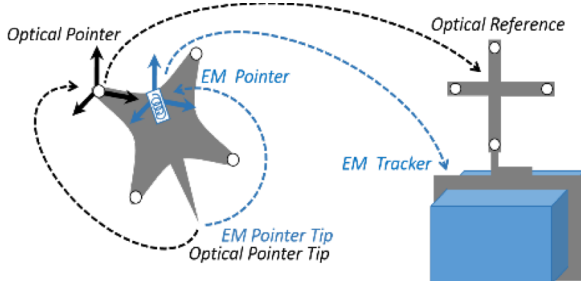


Figure 2. A coordinate system model showing the dual-modality pointer and optical reference.



Figure 4. A zoomed-in image of the dual-modality pointer showing the multiple pegs available for the attachment of optical markers.

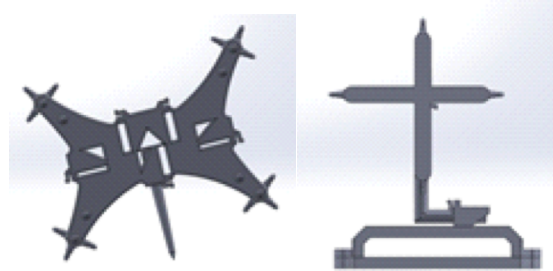


Figure 3. Mechanical design of the rapid prototyped parts shown as screenshots of the .SLDASM files on SolidWorks.

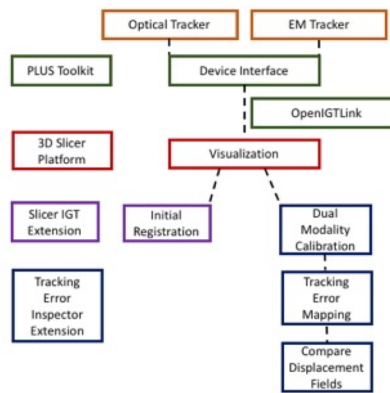


Figure 5. Software architecture diagram of the Tracking Error Inspector.

2.2 3D Slicer module development

In our previous system⁷, several 3D Slicer modules were used in the workflow for measuring and visualizing electromagnetic tracking error. In order to use the previous system, users would have to be familiar with many different functionalities of the 3D Slicer platform, which hindered usability. There was also no dedicated calibration module nor option to measure rotational tracking error. Moreover, users were unable to obtain numerical data regarding tracking error without using 3D Slicer's Transform Visualizer. In order to address these issues, the Tracking Error Inspector extension was developed in the Python programming language. It contains three scripted modules for calibration, mapping, and the comparison of displacement fields (Figure 5).

The new system has a function to calibrate the dual-modality pointer through a streamlined user interface (Figure 6). From the PLUS toolkit, we are able to obtain transformations from the dual-modality pointer to references in both tracking coordinate systems. These transformations are ${}^{EmP}T_{EmT}$ from the EM pointer $\{EmP\}$ to the EM tracker $\{EmT\}$ and ${}^{OpP}T_{OpR}$ from the optical pointer $\{OpP\}$ to the optical reference $\{OpR\}$. A landmark registration was performed in 3D Slicer using Slicer IGT's Fiducial Registration Wizard to obtain a transformation between the EM tracker and optical reference, ${}^{EmT}T_{OpR}$. In order to calibrate the dual-modality pointer's orientation, a transformation between EM and optical pointers (${}^{EmP}T_{OpP}$) is needed. Since ${}^{OpP}T_{OpR} * {}^{EmP}T_{OpP} = {}^{EmP}T_{EmT} * {}^{EmT}T_{OpR}$ forms an AY = XB problem, hand-eye calibration techniques can be used to solve for the unknown ${}^{EmP}T_{OpP}$ transformation¹⁰. Users can specify how many points they would like to collect to be used in the calibration process. After the pointer is moved through space with six degrees of freedom, twenty iterations of a least-squares optimization algorithm are used to optimize the transformations between the electromagnetic and optical pointers (${}^{EmP}T_{OpP}$), and the electromagnetic tracker to optical reference (${}^{EmT}T_{OpR}$). Hence, it is

now also possible to calibrate the pointer orientation using optical and electromagnetic tracking data, thereby allowing us to measure orientation error. Tracking error is measured at the location of the electromagnetic sensor as opposed to the tip of the pointer. This gives the most consistent result because most of the tracking error occurs due to the electromagnetic field distortion at the sensor.

Once the dual-modality pointer is calibrated, users can proceed to map a region of interest (ROI) for position and rotational tracking error. In a simple graphical user interface, users select which transformation they wish to use as a ground truth transformation and which transformation to use as the mapped transformation from a dropdown menu (Figure 7). Similar to our previous system, 3D models such as cubes are generated to indicate to the user where data is collected. Our system can be configured to utilize 3D Slicer's Watchdog module, notifying users when a transformation stops updating. This feature is especially useful to warn users when they are occluding any of the optical markers during the mapping process. Finally, users can also specify output transforms for position and rotational tracking errors and export them as either transforms or .NRRD files.

The final module in the Tracking Error Inspector is the Compare Displacement Fields module. This module allows users to load .NRRD files saved from the mapping procedure and perform simple operations such as averaging and determining the difference between displacement fields. For more complex operations, Matlab can be used once the .NRRD files have been loaded in.

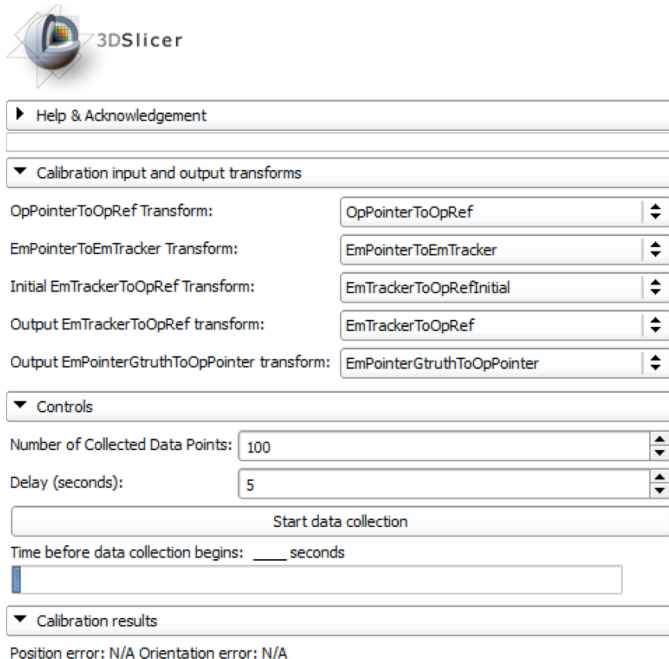


Figure 6. A screenshot of the graphical user interface of the Dual Modality Calibration module in the Tracking Error Inspector extension for 3D Slicer.

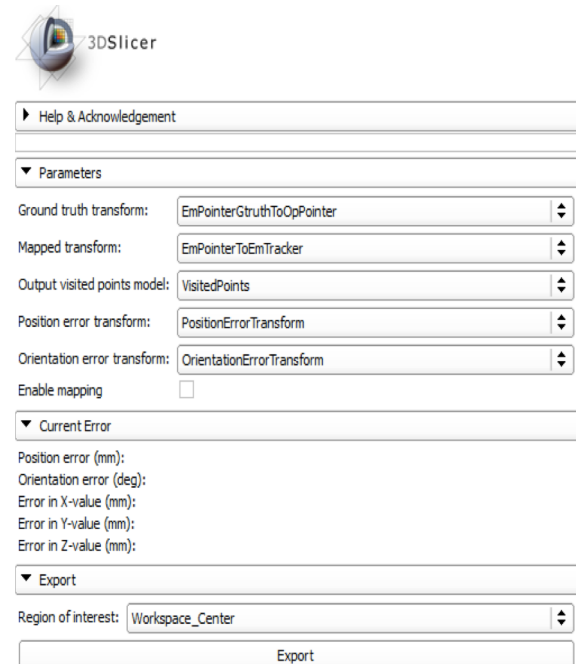


Figure 7. A screenshot of the graphical user interface of the Tracking Error Mapping module in the Tracking Error Inspector extension for 3D Slicer.

2.3 Testing

We tested our system in an operating room that is currently used for navigated lumpectomy procedures (Figure 8). The first round of tests was done in a “clean field”, with the anesthesia machine and electrosurgical cautery powered off, in a region of interest (ROI) away from both machines and the operating table. We also tested the difference between free-hand data sampling and systematic data sampling using a positioning stage and a predefined sampling pattern. The sampling pattern, a meandering spiral, measured 25.5 x 25.5 x 15 cm (length, width, height). There was a distance of 2 cm between parallel planes. When potential sources of tracking error were introduced into the field, two types of tests were performed. The dual-modality pointer was kept stationary and error sources such as the anesthesia machine were moved closer up to a realistic distance. If the tracking error was deemed clinically unacceptable, a freehand mapping was done to gauge if the error varied through the region of the interest. This type of two step testing was done with an electrosurgical cautery and anesthesia machine. In static sampling, we measured the difference in tracker positions and orientations compared to an average of short sequence samples. Testing was done in various positions in the workspace with the cautery off and on. In order to simulate a real patient, a human subject laid on the surgical table. A plastic breast phantom was placed on their chest to simulate the real workspace. The anesthesia machine was powered on and recorded the subject’s heart rate.

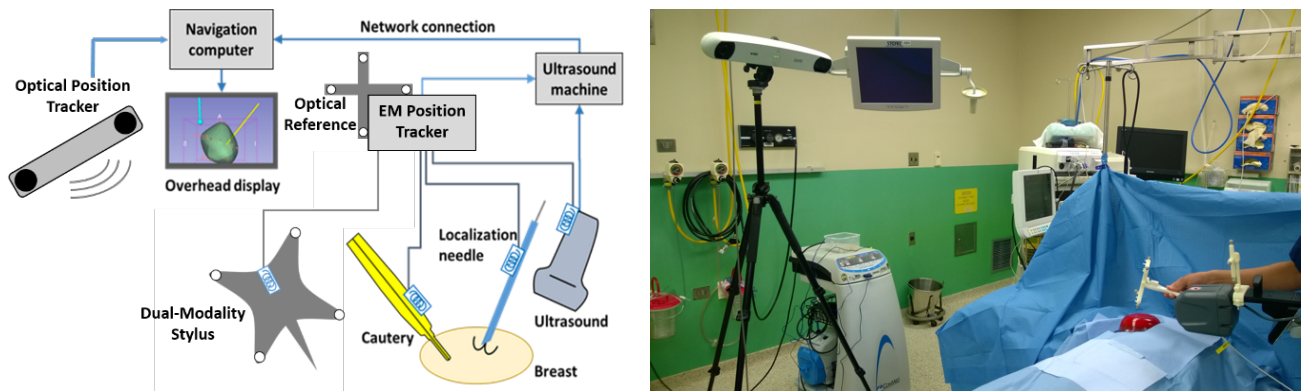


Figure 8. Our system is added to the set-up of the navigated intervention in question for position tracking error measurement. An optical tracker overlooks the workspace, and an optical reference is fixed onto the holder arm of the electromagnetic field generator. A dual-modality pointer is tracked by both trackers.

3. RESULTS AND DISCUSSION

3.1 System performance

Our new calibration module allowed for quick and seamless measurements in a test environment. The entire system can be configured in a few minutes and PLUS configuration files allow users to switch easily between a navigation system and the Tracking Error Inspector. The calibration process is also quick, taking under a minute to perform initial registrations and then obtain the missing transformation between EM and optical pointers (${}^{\text{Emp}}\text{T}_{\text{Opp}}$) using the Dual Modality Calibration module. Even if experimenters believed that they had altered the position of the holder arm of the field generator, the fixed optical reference ensured that the calibration would be able to rapidly correct any changes and allow for accurate measurements. The duration of the mapping procedure is dependent on how densely the user wishes to sample the ROI that they are interested in and its size. For a ROI commonly used in breast surgery (25.5 x 25.5 x 15 cm), we found that in the case of static sampling, a sampling time of thirty seconds seemed to be sufficient to gauge errors. Similarly, in the case of freehand sampling in the same ROI, a sampling time of one to two minutes was sufficient to get a detailed visualization of tracking error. The sampling time duration of systematic sampling can vary, in our case we spent roughly ten minutes mapping the aforementioned ROI in parallel planes. However, despite the large number of data points, the system performed well without crashing and 3D Slicer was able to generate a visualization a short time later (Figure 9).

We were unable to reduce the tracking error of the optical ground truth beyond 0.3 mm. However, it may be possible by increasing the size of the optical markers or printing the tracked tool attachments from a more rigid material to avoid potential deformations. The relative tracking error, or position and orientation of a tool relative to a reference sensor, in clinical environments should also be explored as tracked tools are typically not used without reference sensors.

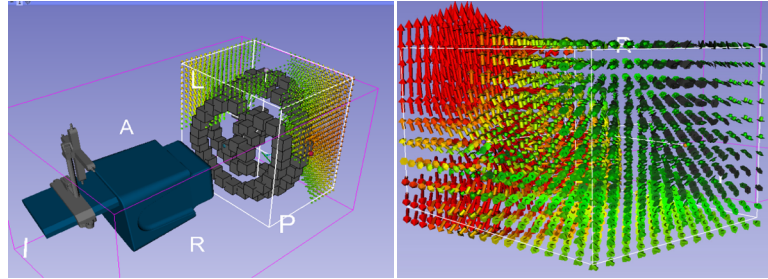


Figure 9. Visualizing the thin-plate-B-spline transform representing the difference between EM and optical positioning readings as glyphs with a 3D model of the Ascension's EM field generator as a reference (left) and a zoomed-in image of the glyphs to indicate the direction of tracking errors (right).

3.2 Findings in breast surgery setup

Table 1. A summary of positional and rotational tracking errors with various surgical equipment and sampling methods. The clinical setup refers to what potential error causing source was tested. Region of interest corresponds to the section of the electromagnetic field generated by the electromagnetic tracker. Positional and rotational errors were calculated by comparing pose and orientation details of the electromagnetic pointer directly through electromagnetic tracking and a chain of transforms that incorporate the optical ground truth (Figure 2).

a.)

Clinical setup	Sampling method	Region of interest	Position error (mean absolute difference, mm)	Orientation error (mean absolute difference, degrees)
Clean field	Systematic	Full	1.32	0.41
Clean field	Systematic	Centre	0.90	0.31
Clean field	Systematic	Periphery	1.93	0.58
Surgical table	Systematic	Center	1.86	0.80

b.)

Clinical setup	Sampling method	Region of Interest	Position error (mean absolute difference, mm)	Orientation error (mean absolute difference, degrees)
Cautery	Static	Periphery	0.21	0.04
Anesthesia machine	Static	Periphery	0.24	0.08

c.)

Clinical setup	Sampling method	Region of Interest	Position error (mean absolute difference, mm)	Orientation error (mean absolute difference, degrees)
Clean field	Freehand	Periphery	0.89	0.39
Surgical table	Freehand	Periphery	1.23	0.35
Anesthesia machine	Freehand	Periphery	1.68	0.39

We found that the tracking error is up to 2 mm and is not strongly affected by the presence of a surgical table, anesthesia equipment, or electrosurgical cautery device (Table 1a.). Even in a clean field with all surgical or anesthesia equipment located several meters away, there may be a large discrepancy between tracking accuracy in the center of a field as compared to the periphery of the field. Freehand sampling also suggests tracking accuracy was poorer in the periphery of a field (Table 1c.). When the cautery was moved near the stationary, dual-modality pointer and was turned on, no change was detectable in position or orientation. We believe that this may be due to differences in operating frequency between the electrosurgical cautery and EM tracking system. Thus, no complete mapping was warranted. Likewise, when the anesthesia machine was placed at a realistic distance of 1.5 m away from the field generator, as suggested by a consulting surgeon, experimenters determined that the tracking accuracy was not overtly impacted (Table 1b, c.).

4. CONCLUSION

Various improvements were made to our presented system for the measurement and visualization of electromagnetic tracking error. The 3D printing of dedicated tools and the development of open-source software modules for pointer calibration in both position and orientation allows for more accurate measurement of electromagnetic tracking error. We explored potential sources of errors in the navigated lumpectomy setup proposed by Ungi *et al.*⁴, to test whether our system can be used under realistic motions in operating room environments. We found that surgical and anesthesia equipment may be moved to a sufficient distance as to not interfere with tracking or the anesthesia procedure. The positioning of the electromagnetic field generator is also crucial towards minimizing tracking error. As our system is applicable to a variety of use cases, further tests may be done with different electromagnetic sensors and in different surgical setups. We hope that the presented system will be easy to reproduce by others, contributing to better safety and feasibility tests before navigation systems are used in patients.

5. CURRENT WORK

5.1 In-Vivo testing

Recently, our ethics approval has been extended for further clinical testing of the LumpNav system. During these future tests we hope to use this system to verify the accuracy of EM tracking during crucial moments in the workflow. Examples of these moments include before the procedure begins as well as before the tumor is segmented for navigation.

5.2 Redundant sensing

Since our system relies on an external optical tracker as the source of the ground truth, three issues may come forward once testing begins in-vivo. Optical trackers rely on a clear line-of-sight with their corresponding markers, which can be challenging to ensure in a typically crowded operating room. In terms of cost, optical trackers such as the Polaris are much more expensive than adding a second EM tracker. Furthermore, although the PLUS toolkit and OpenIGTLINK allow for relatively seamless transitions between the LumpNav and Tracking Error Inspector systems, there is still a degree of disruption to the surgeon's workflow in order to gain feedback on tracking accuracy. All of these issues prevent surgeons from receiving constant updates on potential EM field distortion. However, using redundant sensing in a method similar to Sadjadi *et al.*¹¹ and Vaccarella *et al.*¹², it is possible to have real-time measurements throughout the procedure. Several EM sensors would be placed on a rapid-prototyped frame, and this frame would be fixed onto the patient's breast under the drape. A sensor fusion algorithm would combine their readings to provide an estimate of the tracking accuracy at the center of this frame. This tracking accuracy reading could then be displayed on the main navigation computer of the LumpNav system. In cases where this estimate of tracking error is clinically unacceptable, the surgical team could bring the Tracking Error Inspector system into the workspace to perform a detailed analysis to determine the source of field distortion and deal with it appropriately.

6. ACKNOWLEDGMENTS

This work was supported in part through the Applied Cancer Research Unit program of Cancer Care Ontario with funds provided by the Ontario Ministry of Health and Long-Term Care. Gabor Fichtinger was supported as a Cancer Care Ontario Research Chair in Cancer Imaging. Vinyas Harish was supported by the Summer Work Experience Program (SWEP) at Queen's University.

7. REFERENCES

- [1] Krücker, J., Xu, S., Glossop, N., Viswanathan, A., Borgert, J., Schulz, H., and Wood, B.J., "Electromagnetic Tracking for Thermal Ablation and Biopsy Guidance: Clinical Evaluation of Spatial Accuracy," *Journal of Vascular and Interventional Radiology* 18(9), 1141-1150 (2007).
- [2] Feuerstein, M., Reichl, T., Vogel, J., Traub, J., and Navab, N., "New Approaches to Online Estimation of Electromagnetic Tracking Errors for Laparoscopic Ultrasonography," *Computer aided surgery: official journal of the International Society for Computer Aided Surgery* 13(5), 11-23 (2008).
- [3] Lugez, E., Sadjadi, H., Pichora, D.R., Ellis, R.E., Akl, S.G., and Fichtinger, G., "Electromagnetic tracking in surgical environments: usability study," *International Journal of Computer-Assisted Radiology and Surgery* 10(3), 253-62 (2015).
- [4] Ungi, T., Gauvin, G., Lasso, A., Yeo, C., Pezeshki, P., Vaughan, T., Carter, K., Rudan, J., Engel, C., and Fichtinger, G., "Navigated breast tumor excision using electromagnetically tracked ultrasound and surgical instruments," *Biomedical engineering, IEEE Transactions on*, to appear (2015).
- [5] Hwang, E.S., "Breast conservation: Is the survival better for mastectomy?," *Journal of Surgical Oncology* 110(1), 58-61 (2014).
- [6] Mullen, R., Macaskill, E.J., Khalil, A., Elseedawy, E., Brown, D.C., Lee, A.C., Purdie, C.A., Jordan, L.B., and Thompson, A.M., "Involved anterior margins after breast conserving surgery: is re-excision required?," *European Journal of Surgical Oncology* 38(4), 302-306 (2012).
- [7] Harish, V., Ungi, T., Lasso, A., MacDonald, A., Nanji, S., and Fichtinger, G., "Intraoperative measurement and visualization of electromagnetic tracking error," *Proc. SPIE* 9415, 94152H (2015).
- [8] Lasso, A., Heffter, T., Rankin, A., Pinter, C., Ungi, T., and Fichtinger, G., "PLUS: open-source toolkit for ultrasound-guided intervention systems," *Biomedical engineering, IEEE Transactions on* 61(10), 2527-37 (2014).
- [9] Tokuda, J., Fischer, G.S., Papademetris, X., Yaniv, Z., Ibanez, L., Cheng, P., Liu, H., Blevins, J., Arata, J., Golby, A.J., Kapur, T., Pieper, S., Burdette, E.C., Fichtinger, G., Tempany, C.M., and Hata, N., "OpenIGTLINK: an open network protocol for image-guided therapy environment," *International Journal of Medical Robotics and Computer Assisted Surgery* 5(4), 423-434 (2009).
- [10] Strobl, K.H., and Hirzinger, G., "Optimal hand-eye calibration," *Proc. IEEE/RSJ International Conference on Intelligent Robots and Systems*, 4647-4653 (2006).
- [11] Sadjadi H., Hashtrudi-Zaad, K., and Fichtinger, G., "Simultaneous Electromagnetic Tracking and Calibration for Dynamic Field Distortion Compensation," *Biomedical Engineering, IEEE Transactions on*, to appear (2015).
- [12] Vaccarella A., De Momi, E., Enquobahrie, A., and Ferrigno, G., "Unscented Kalman Filter Based Sensor Fusion for Robust Optical and Electromagnetic Tracking in Surgical Navigation," *Instrumentation and Measurement, IEEE Transactions on*, 62(7), 2067-2081 (2013).